

## Evolution of poling-assisted bleaching of metal-doped nanocomposite glass with poling conditions

Olivier Deparis<sup>a)</sup>

*Electromagnetism and Telecommunications Department, Faculté Polytechnique de Mons, B-7000 Mons, Belgium*

Peter G. Kazansky

*Optoelectronics Research Centre, University of Southampton SO17 1BJ, United Kingdom*

Alexander Podlipensky, Amin Abdolvand, Gerhard Seifert, and Heinrich Graener

*Optics Group, Physics Department, Martin-Luther-University Halle-Wittenberg, D-06099 Halle, Germany*

(Received 26 August 2004; accepted 23 May 2005; published online 23 June 2005)

Poling-assisted bleaching was studied with respect to poling time, voltage, and temperature in glass samples having a gradient of silver nanoparticles across the depth. The optical extinction band due to the particles' surface plasmon resonance (around 415 nm) was measured and the Maxwell-Garnett effective medium theory was used to fit extinction spectra. Fitting allowed us to determine the evolution of the thickness of the near-surface layer where the particles' volume filling factor has dropped to zero as a result of the bleaching process. At 280 °C, bleaching started with a voltage as low as 200 V and saturated with time after about 1 h. Tight glass-electrode contact, voltage of at least 1 kV, and temperature higher than 200 °C were required in order to obtain significant and uniform bleaching in the poled area. The results were discussed in terms of the underlying electric-field-assisted dissolution of embedded metal nanoparticles. © 2005 American Institute of Physics. [DOI: 10.1063/1.1977205]

Glasses containing metal nanoparticles are promising materials for various applications because of their unique linear and nonlinear optical properties which are mainly determined by the surface plasmon resonance of embedded nanoparticles<sup>1</sup>. The surface plasmon resonance (SPR) can be tailored by choosing appropriately both the metal and the glass host, and by controlling the size, shape, concentration, and distribution of metal clusters.<sup>2</sup> Recently, we discovered that thermal poling—i.e., treatment under dc electric field at elevated temperature—was capable of bleaching Ag-doped nanocomposite glass up to complete transparency.<sup>3</sup> Depending on the volume filling factor and the shape of nanoparticles, either complete or partial bleaching of the glass was demonstrated<sup>3</sup>. Transparency was achieved in samples with ellipsoidal Ag particles uniformly distributed in  $\sim 1\text{-}\mu\text{m}$ -thick layer after poling at 280 °C and 1 kV whereas partial bleaching was achieved in samples with spherical Ag particles and a gradient of the filling factor for the same poling conditions.<sup>3</sup> (In latter samples, voltages higher than 3 kV were needed to reach transparency.<sup>4</sup>) The underlying physical mechanism has been identified as the electric-field-assisted dissolution of embedded metal nanoparticles.<sup>3,4</sup> This technique has already proven to be useful for the realization of millimeter-size sharp-edge transparent areas,<sup>3</sup> micron-size structured bleaching patterns,<sup>4</sup> and large colored areas.<sup>5</sup> In early experiments, we were not able to determine at which voltage step (voltage was increased step by step up to 1 kV) the bleaching appeared and how much time it took to complete. Moreover, experiments were performed at a fixed temperature (280 °C in Ref. 3). The aim of this letter is to study the evolution of poling-assisted bleaching in Ag-doped nanocomposite glass with poling conditions. Samples having a

gradient of spherical Ag nanoparticles across the depth were poled using various combinations of voltage, time, and temperature. We found that bleaching had a voltage threshold, saturated with time and required voltage of at least 1 kV and temperature higher than 200 °C in order to be significant and uniform in the poled area.

The samples under test (1 mm thick) were prepared from a soda-lime float glass by  $\text{Ag}^+ - \text{Na}^+$  ion exchange and subsequent thermal annealing in  $\text{H}_2$  reducing atmosphere.<sup>6</sup> Spherical Ag nanoparticles (30–40 nm diameter) were aggregated in a 6- $\mu\text{m}$ -thick near-surface layer with a volume filling factor ( $f = V_{\text{Ag}}/V_{\text{total}}$ ) which decreased exponentially across the depth.<sup>4</sup> Thermal poling was carried out in air inside an oven using pressed-contact steel electrodes ( $6 \times 9 \text{ mm}^2$ ). A first sample was successively poled at 280 °C with various voltage-time combinations: 200 V–10, –10, –20, –40 min; 10 min–400 V, –600, –800 V; 15 min–1 kV. Six additional samples were poled at various temperatures (150, 190, 220, 250, 280, 300 °C). In the latter case, the voltage was increased by steps of 200 V (10 min each) up to 1 kV for the sake of comparison with previous experiments<sup>3</sup>. After poling, microscope images of the sample (in transmission mode) were recorded and the optical extinction spectrum [ $E = -\ln(I_{\text{out}}/I_{\text{in}})$ ,  $I$ : light intensity] was measured using an UV-visible-near-infrared spectrometer and a 2 mm diameter aperture which was located in uniformly bleached region of the sample. Within the SPR wavelength range (visible range for spherical Ag nanoparticles in a soda-lime glass), the extinction spectrum of metal-doped nanocomposite glass can be calculated from the Maxwell-Garnett effective medium theory

<sup>a)</sup>Electronic mail: olivier.deparis@fpms.ac.be

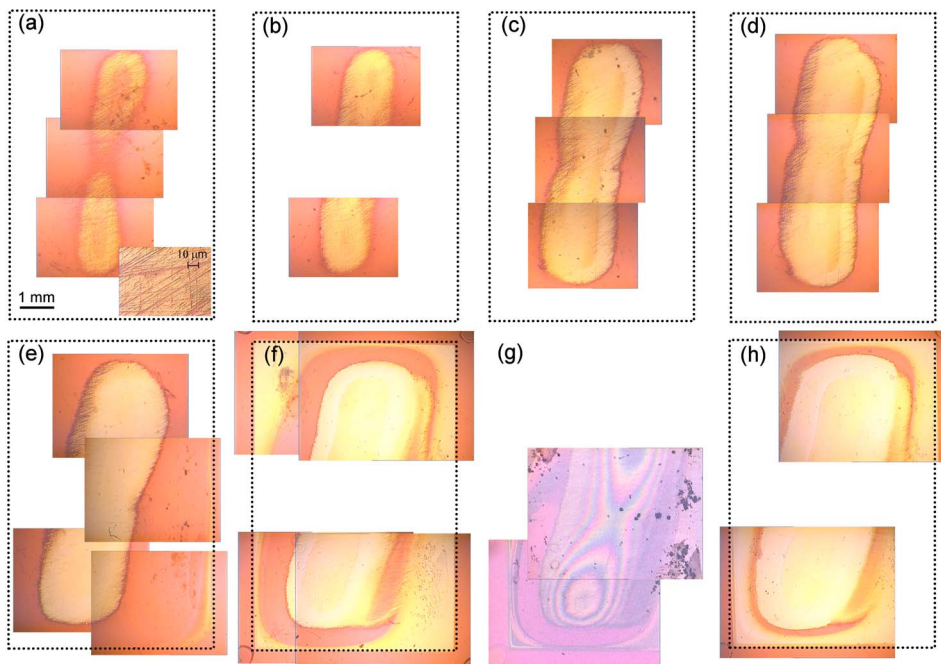


FIG. 1. (Color online) Microscope images (in transmission) of a Ag-doped nanocomposite glass sample after successive poling steps at 280 °C: 200 V–10 (a), –10 (b), –20 (c), –40 min (d); 10 min–400 V (e), –600 (f), –800 V (h). Zones where Ag nanoparticles were dissolved appear yellowish. Dotted rectangles represent the electrode. The microscope image (in reflection) taken from the sample's cathode side while the anode stuck on the glass surface is also shown (g). Images (a)–(h) were taken using 2× objective. Zoomed image in (a): 50× objective.

$$E = \frac{2\omega}{C} \int_0^L \left\{ \text{Im} \left[ \sqrt{\varepsilon_h \frac{(\varepsilon_i + 2\varepsilon_h) + 2f(x)(\varepsilon_i - \varepsilon_h)}{(\varepsilon_i + 2\varepsilon_h) - f(x)(\varepsilon_i - \varepsilon_h)}} \right] \right\} dx, \quad (1)$$

where the expression under the square root is the effective (complex) dielectric function  $\varepsilon_{\text{eff}}(\omega)$ ,  $L$  is the sample thickness,  $C$  is the speed of light,  $\omega$  is the angular frequency, and  $\varepsilon_i$  and  $\varepsilon_h$  are the dielectric constants of metal and host material, respectively. The complex function  $\varepsilon_i$  was calculated using the Drude model of a metal:  $\varepsilon_i(\omega) = \varepsilon_b + 1 - \omega_p^2 / (\omega^2 + i\gamma\omega)$ , where  $\varepsilon_b$  is the bound electron dielectric constant,  $\gamma$  is the damping frequency of electron oscillations, and  $\omega_p$  is the free electron plasma frequency. In the case of silver,  $\hbar\omega_p = 9.2$  eV and the function  $\varepsilon_i(\omega)$  is well approximated, within the wavelength range of interest, by taking  $\varepsilon_b = 4.0$  and  $h\gamma = 0.5$  eV.<sup>7</sup> We took  $\varepsilon_h = 2.23$  for the host glass. Since bleaching proceeded “layer-by-layer” from top surface (see discussion later), we defined  $d$  as the thickness of the bleached layer and we took  $f(x) = 0$  for  $0 \leq x < d$ . In unbleached layers ( $d \leq x \leq L$ ) we took  $f(x) = f_0 \exp(-x/w_f)$ . The values of  $f_0$  and  $w_f$  were determined by fitting the extinction spectrum of pristine sample using Eq. (1) and  $d = 0$ . The value of  $d$  after the poling treatment was determined by fitting the extinction spectrum of bleached sample using Eq. (1) and  $d$  as free parameter.

At a poling temperature of 280 °C, bleaching occurred with voltage as low as 200 V but did not cover the entire electrode area [Figs. 1(a)–1(d)]. Bleaching started in a central zone which covered ~13% of the total electrode area after 10 min of poling; this zone extended only slightly with increasing poling time. After a 10 min poling step at 400 V [Fig. 1(e)], bleaching started near the electrode edges as well. After two 10 min poling steps at 600 and 800 V, respectively [Figs. 1(f) and 1(h)], the bleached zones in the middle and near the edges tended to merge progressively. Finally, after a 15 min poling step at 1 kV, the entire area underneath the electrode was bleached (not shown). These observations revealed the role of the glass-electrode contact in the bleaching process. Mechanically pressed electrodes did not provide

uniform contact with the sample surface over the entire electrode area and the bleached zones were therefore associated with tight contact. Evidence of this effect was found when the sample was probed in reflection from the cathode side just after the poling step at 600 V while the anode stuck on the glass surface due to electrostatic forces [Fig. 1(g)]. Clearly, areas where tight contact was achieved (see Newton rings) corresponded to the bleached zones. More evidence was given by the observation of dark orange lines (unbleached glass) crossing yellowish zones (bleached glass) which turned out to be a replica of scratches on the electrode surface [Fig. 1(a), zoomed image]. As we demonstrated recently, one can take advantage of this contact effect to produce microstructured bleaching patterns.<sup>4</sup> At 280 °C, bleaching occurred with voltages lower than 1 kV but the strength of the SPR band was so high that its peak could not be measured [Figs. 2(b) and 2(c)], as in the pristine sample [Fig. 2(a)]. After poling up to 1 kV, however, the entire band could be measured, revealing a SPR peak at ~415 nm [Fig. 2(d)]. Using a voltage of 1 kV, bleaching occurred in the temperature range from 150 to 300 °C [Figs. 2(f) and 2(g)]. Bleaching became visually evident only at temperatures above

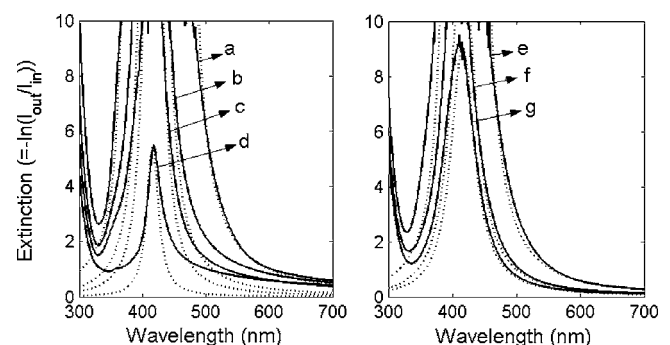


FIG. 2. Extinction spectra of the Ag-doped nanocomposite glass (solid curves): as-received samples (a), (e); sample poled at 280 °C with successive time-voltage steps: after 40 min–200 V step (b), after 10 min–600 V step (c), after 15 min–1 kV step (d); samples poled up to 1 kV at various temperatures: 220 (f), 280 °C (g). Dotted curves are best fits to Eq. (1).

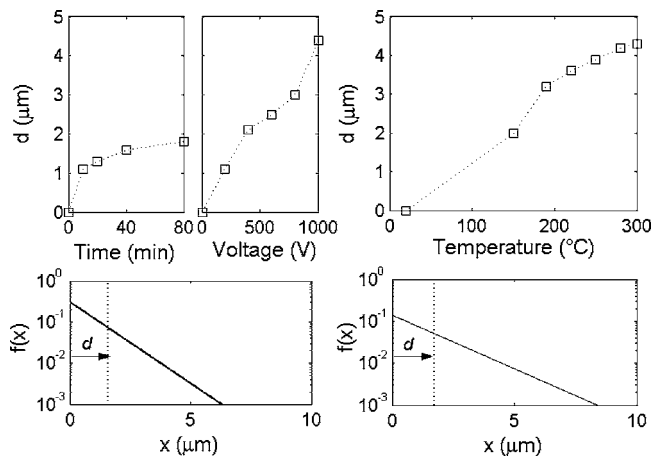


FIG. 3. Thickness of the bleached layer as a function of the poling time, voltage, and temperature (top charts), and depth gradient of the particle's volume filling factor in pristine samples (bottom charts). The values of  $d$  were obtained by fitting extinction spectra to Eq. (1).

190  $^{\circ}\text{C}$  and the SPR peak was detectable only at temperatures above 280  $^{\circ}\text{C}$  [Fig. 2(g)]. Samples could not be poled above 300  $^{\circ}\text{C}$  because of the current runaway due to high ionic conductivity of the host glass. By fitting measured extinction spectra, the evolution of  $d$  with poling time, voltage, and temperature was determined (Fig. 3). Knowing the value  $d$ , the filling factor subsisting at depths  $x \geq d$  can be calculated (Fig. 3)

The evolution of bleaching with poling conditions can be explained in terms of the underlying electric-field-assisted dissolution of embedded metal nanoparticles or clusters.<sup>3,4</sup> Both ionic and electronic conduction must be taken into account here. In silicate glass, thermally activated migration of mobile ions (such as  $\text{Na}^+$ ) leads to the formation of an ion-depleted layer underneath the anode where a high electric field builds up.<sup>8</sup> In our samples the mechanism may be slightly different because of the quite different spatial distribution of mobile ion impurities after the  $\text{Na}^+/\text{Ag}^+$  ion-exchange process, as compared to the original soda-lime substrate. But in any case there will be a strong field enhancement in the vicinity of the silver clusters. On the other hand, as soon as the threshold for ionization of the silver clusters is exceeded, electrons move towards the anode and silver ions, which are ejected from the ionized clusters due to strong Coulomb forces, drift away in the depth. Since the silver clusters in regions of a higher filling factor (closer to the surface in our samples) are ionized first, the dissolution proceeds layer-by-layer from the top surface. Note that both the release of  $\text{Ag}^+$  and the injection of  $\text{H}_3\text{O}^+$  or  $\text{H}^+$  from the atmosphere (at the anode) should be taken into account for a more complete description of the ion depletion process. At 280  $^{\circ}\text{C}$ , a voltage as low as 200 V was sufficient to complete dissolution of Ag nanoparticles in a 1- $\mu\text{m}$ -thick layer after 10 min (Fig. 3). Remarkably, the depth of the bleached layer is of the same order as the thickness of ion-depleted layer. At 280  $^{\circ}\text{C}$  and 1 kV, the former was estimated to 4.4  $\mu\text{m}$  (Fig. 3) whereas the latter was estimated to  $\sim 4.0 \mu\text{m}$  from the  $\text{Na}^+$  depth profile previously measured

using x-ray element analysis.<sup>4</sup> Our results also showed that the bleached layer (at least up to 1 kV) was thinner than the thickness of the Ag-doped layer in pristine samples. Therefore, incomplete bleaching (and its saturation with time) can be explained by the presence of particles which are located deeper in the depth with a smaller filling factor, where the local electric field strength is not high enough to cause their dissolution. As the voltage is increased, the electric field increases in strength and extends deeper in the sample (the actual field distribution depends on the ion depletion and metal cluster distributions in a nontrivial way). Both the higher local field strength and the extension of the field distribution contribute to dissolve those silver particles which remain deeper in the glass. The increase of  $d$  with temperature, on the other hand, is consistent with the thermally activated nature of the ion migration process. The role of the glass-electrode contact can be understood if we remind that electrons ejected from ionized clusters have to be extracted at the anode. The pictures in Fig. 1 suggest that tight contact is needed to extract electrons efficiently. Moreover, the electrostatic force exerted on the sample is considerably enhanced due to the buildup of an intense dc field underneath the anode during poling, which results in an enhanced contact. A last remark concerns the fitting of extinction spectra. For pristine samples, best fits were obtained by taking  $h\nu = 0.5 \text{ eV}$  whereas, for poled samples, we had to take  $h\nu = 1.0 \text{ eV}$  (Fig. 2, left) or 2.0 eV (Fig. 2, right) in order to improve fit quality. The resulting broader SPR band can be interpreted, in terms of Mie's scattering theory,<sup>1</sup> as a decrease of particle's (mean) diameter, here from 30–40 nm to less than 10 nm.<sup>1</sup> For those particles subsisting in glass after poling, it means that only a fraction of the silver ions was ejected from the cluster.

In conclusion, bleaching of Ag-doped nanocomposite glass was studied with respect to poling time, voltage, and temperature, and the corresponding evolution of the thickness of the bleached layer was determined. The results were useful to understand more deeply the underlying nanoparticle dissolution process.

The authors are very grateful to CODIXX AG in Barleben (Germany) for providing the samples. One of the authors (O.D.) acknowledges the IAP V/18 program of Belgian Science Policy.

<sup>1</sup>U. Kreibig and M. Vollmer, *Optical Properties of Metal Clusters* (Springer, Berlin, 1995).

<sup>2</sup>K. L. Kelly, E. Coronado, L. L. Zhao, and G. C. Schatz, *J. Phys. Chem. B* **107**, 668 (2003).

<sup>3</sup>O. Deparis, P. G. Kazansky, A. Abdolvand, A. Podlipensky, G. Seifert, and H. Graener, *Appl. Phys. Lett.* **85**, 872 (2004).

<sup>4</sup>A. Podlipensky, A. Abdolvand, G. Seifert, H. Graener, O. Deparis, and P. G. Kazansky, *J. Phys. Chem. B* **108**, 17699 (2004).

<sup>5</sup>A. Abdolvand, A. Podlipensky, G. Seifert, H. Graener, O. Deparis, and P. G. Kazansky, *Opt. Express* **13**, 1266 (2005).

<sup>6</sup>K.-J. Berg, A. Berger, and H. Hofmeister, *Z. Phys. D: At., Mol. Clusters* **20**, 309 (1991).

<sup>7</sup>P. B. Johnson and R. W. Christy, *Phys. Rev. B* **6**, 4370 (1972).

<sup>8</sup>P. G. Kazansky and P. St. J. Russel, *Opt. Commun.* **110**, 611 (1994).